IIETA International Information and Engineering Technology Association
Advancing the World of Information and Engineering

Journal Européen des Systèmes Automatisés
Vol. 59, No. 5, May, 2026, pp. 1263-1274
Journal homepage: http://iieta.org/journals/jesa

Swarm Robot Communication Using ESP-NOW Mesh Protocol for Multi-Agent Coordination in Indoor Navigation

Deosa Putra Caniago[1*], Luki Hernando[1], Ririt Dwiputri Permatasari[2], M. Ansyar Bora[3], Aulia Agung Dermawan[3], Alhamidi[2], Andrian Syah[1], Surya Tirta Chandra[1]

[1] Computer Engineering Department, Faculty of Information Technology, Institut Teknologi Batam, Batam 29425, Indonesia
[2] Information Systems Department, Faculty of Information Technology, Institut Teknologi Batam, Batam 29425, Indonesia
[3] Engineering Management Department, Faculty of Industrial Technology, Institut Teknologi Batam, Batam 29425, Indonesia

Corresponding Author Email: deosa@iteba.ac.id

https://doi.org/10.18280/jesa.590507

Received: 2 March 2026
Revised: 27 April 2026
Accepted: 15 May 2026
Available online: 31 May 2026

Keywords:
Enhanced Peer-to-Peer Network, formation stability, indoor navigation, IoT-based robot communication, multi-agent coordination, swarm robotics

ABSTRACT

Swarm robotics offers a scalable, decentralized approach for collective task execution; however, its indoor implementation remains constrained by communication stability and inter-agent synchronization. This study proposes and realizes an Internet of Things (IoT)-based swarm robot communication framework using the Enhanced Peer-to-Peer Network (ESP-NOW) mesh protocol for multi-agent indoor navigation. Each robot is designed as a mobile IoT node equipped with ultrasonic sensing, inertial orientation monitoring, and differential-drive actuation, enabling real-time peer-to-peer data exchange without reliance on external network infrastructure such as routers or access points. Experimental evaluations were conducted using 3, 5, and 7 robots under three indoor navigation scenarios: straight corridor, obstacle-centered path, and split-path environments. Performance metrics included Packet Delivery Ratio (PDR), communication latency, Received Signal Strength Indicator (RSSI), and Formation Stability Index (FSI). Results demonstrate that the proposed system achieves high communication reliability with PDR values above 98% for three robots and above 95% for five robots, while maintaining PDR above 92% for seven robots. Communication latency remains below 20 ms for three robots and below 40 ms for seven robots. RSSI measurements indicate a practical indoor communication range of approximately 8–10 m, and FSI values of 0.955, 0.910, and 0.840 were obtained for 3, 5, and 7 robots, respectively, indicating stable to highly stable formation control. These findings confirm that ESP-NOW Mesh communication is a lightweight, energy-efficient, and reliable protocol for small-to-medium indoor swarm robotic systems, and provides a reproducible foundation for scalable IoT-based collaborative robotics.

1. INTRODUCTION

The development of robotics technology has shown a very significant increase over the past two decades, driven by a growing tendency toward more intelligent, collaborative, and adaptive system designs capable of operating in dynamic environments [1]. One rapidly evolving field within this domain is swarm robotics, a multi-robot approach inspired by the social behaviors of biological organisms such as ants, bees, and fish, which accomplish collective tasks through local interactions and self-organization [2, 3]. This approach offers scalability, redundancy, and high fault tolerance, as the system does not rely on a single centralized controller [4]. When one agent fails, other agents can compensate, allowing the mission to continue collectively and efficiently [5, 6].

On the other hand, the rapid advancement of the Internet of Things (IoT) has enabled physical devices to communicate and exchange data wirelessly in real time for monitoring and adaptive control purposes [7]. Initially applied to static sensor networks, IoT has evolved into IoT-based robotic systems, in which robots act as mobile IoT nodes that perform not only sensing and actuation but also intelligent inter-unit communication [8, 9]. The integration of IoT and robotics has given rise to the paradigm of IoT-based swarm robotics, which enables the emergence of collective intelligence through distributed network architectures [10, 11]. This paradigm forms the foundation of cyber-physical swarm systems capable of performing navigation, environmental mapping, and mission coordination in a decentralized manner [12].

Nevertheless, the implementation of swarm robotics in indoor environments still faces significant challenges, particularly in terms of inter-robot communication. Conventional Wi-Fi technology requires access points and suffers from limitations in the number of simultaneous connections [13]. Bluetooth provides limited bandwidth and short communication range, which are insufficient for high-speed swarm data exchange [14, 15]. Meanwhile, LoRa excels in long-range communication but is unsuitable for real-time multi-robot coordination due to its very low throughput capacity [16]. These limitations highlight the need for

communication protocols that operate without infrastructure, offer low latency, consume minimal energy, and support a large number of nodes for indoor swarm operations [17, 18].

One communication protocol that has recently attracted increasing attention is Enhanced Peer-to-Peer Network (ESP-NOW), a low-power, low-latency communication protocol based on ESP32 that enables peer-to-peer data exchange without routers or internet connectivity [19]. Its advantages, including small packet size, low energy consumption, and multi-node communication support, make ESP-NOW highly promising for swarm robotics applications [20, 21]. Unlike conventional swarm communication frameworks that rely on centralized network infrastructure, the proposed ESP-NOW Mesh model emphasizes full decentralization with peer-to-peer synchronization. This design choice positions the proposed system as one of the first implementations focusing on infrastructure-free real-time swarm coordination in indoor environments. However, most existing ESP-NOW-based studies still focus on static IoT sensors, environmental monitoring, or single-node usage rather than dynamic communication among mobile robots [22]. Research on the application of ESP-NOW in multi-agent mesh schemes for indoor navigation remains very limited, particularly with respect to latency evaluation, packet delivery ratio (PDR), Received Signal Strength Indicator (RSSI) degradation, and formation accuracy [23, 24].

Furthermore, many studies on indoor swarm robotics reported in the literature remain dominated by simulations and lack real-hardware implementations operating under actual conditions [25]. In practice, signal interference, multipath fading, room geometry, and robot motion dynamics represent critical factors that cannot be fully captured through digital simulations alone [26, 27]. Therefore, experimental evaluations based on real implementations are far more relevant for understanding network stability, coordination reliability, and navigation performance under realistic conditions [28]. This real-hardware experimental emphasis distinguishes the proposed study from simulation-dominated swarm research and strengthens the empirical validity of the obtained performance results.

Based on these research gaps, this study proposes the development and evaluation of an IoT-based swarm robot system using the ESP-NOW Mesh communication protocol for multi-agent coordination in indoor navigation. Each robot functions as a mobile IoT node that exchanges real-time information related to position, movement direction, and sensor status. Experimental evaluations are conducted to measure PDR, communication latency, RSSI, and formation success across various indoor scenarios [29, 30]. With this perspective, the proposed framework contributes not only as a communication solution but also as a benchmark architecture for future IoT-based swarm robotic research. Consequently, this work provides not only technical contributions to the implementation of IoT-based swarm robots but also opens new research directions toward more scalable distributed multi-robot systems suitable for real operational environments [31-33].

This research is expected to serve as a foundation for the development of large-scale IoT-based swarm robotics systems for indoor monitoring, warehouse automation, building exploration, and disaster victim search operations [34]. In addition to providing a lightweight and efficient communication framework, the results of this study also create opportunities for the development of more adaptive, intelligent, and artificial intelligence-oriented coordination algorithms in future research.

Beyond experimental validation, the results of this study also provide practical design guidelines for implementing decentralized indoor swarm robotic systems based on ESP-NOW Mesh communication. The quantified performance boundaries obtained—such as communication reliability degradation, latency tolerance thresholds, and effective communication range—can be used as reference parameters for designing scalable and reliable IoT-based swarm platforms. Thus, the proposed framework can serve as an engineering benchmark for the development and deployment of indoor swarm systems in various scenarios, particularly warehouse automation, collaborative inspection, and multi-robot building exploration.

The main contributions of this research can be summarized as follows:

1. Development of a decentralized swarm robot communication framework based on the ESP-NOW Mesh protocol for indoor multi-agent coordination.
2. Experimental evaluation of the communication performance using four key metrics: PDR, communication latency, RSSI signal strength, and Formation Stability Index (FSI).
3. Validation of swarm formation stability under multiple indoor navigation scenarios, including straight corridor navigation, obstacle avoidance, and multi-room path splitting.
4. Introduction of the FSI as a practical metric for evaluating formation coordination in real swarm robotic systems.

Table 1. Comparison of communication technologies for multi-robot systems

Technology	Latency	Range	Power Consumption	Suitability
Wi-Fi Mesh	Medium	Medium	High	Multi-robot network
Bluetooth Low Energy (BLE) Mesh	Low	Short	Low	Small Internet of Things (IoT) devices
ZigBee	Medium	Medium	Low	Sensor networks
Enhanced Peer-to-Peer Network (ESP-NOW)	Very low	Medium	Very low	Real-time swarm robotics

Although ESP-NOW has been widely applied in IoT-based communication systems, most existing implementations focus on static sensor networks or single-node communication scenarios. The application of ESP-NOW in dynamic multi-robot systems, particularly for real-time swarm coordination in indoor environments, remains relatively unexplored. Therefore, this study aims to investigate the feasibility and performance of ESP-NOW Mesh communication for real swarm robotic platforms operating under indoor navigation conditions. A comparative summary of widely adopted communication technologies for multi-robot systems is presented in Table 1, highlighting their respective characteristics in terms of latency, communication range, power consumption, and suitability for swarm robotic applications.

2. MATERIAL AND METHODS

This study adopts an experimental approach by developing an IoT-based swarm robotic system that employs the ESP-NOW Mesh protocol as the primary communication scheme. This section describes the overall system design, hardware configuration, IoT communication architecture, swarm coordination algorithms, indoor navigation scenarios, and performance evaluation procedures.

2.1 System architecture overview

The proposed swarm robotic architecture is designed based on the concept of distributed IoT nodes, in which each robot operates as an intelligent autonomous unit equipped with sensing, computation, and communication capabilities through ESP-NOW Mesh. The system does not rely on a permanent central controller; instead, formation coordination and navigation decisions are achieved through continuous data exchange among robots within a distributed network.
The system architecture is organized into four main functional layers, as summarized in Table 2.

The proposed IoT-based swarm robotic system architecture is structured into four main functional layers. The Perception Layer serves as the interface between the robot and the physical environment by collecting distance, orientation, and odometry data required to model surrounding conditions in real time. The Networking Layer forms the core of the swarm communication system by handling inter-robot data transmission through ESP-NOW Mesh in a peer-to-peer manner, thereby enabling a distributed network without reliance on external infrastructure. The Decision Layer functions as a local decision-making unit on each robot to determine movement direction, formation control, and navigation trajectories based on collective information received from neighboring swarm nodes. The Actuation Layer is responsible for executing these decisions through Pulse Width Modulation (PWM) signals that control the DC motors, resulting in physical robot motion. This layered architecture allows the system to maintain operational continuity even in the presence of failures in one or more nodes, as no centralized controller exists that could act as a single point of failure. The decentralized approach enables the swarm to adapt dynamically and preserve formation stability during indoor navigation. Table 2 presents the four functional layers of the proposed swarm robotic architecture, including their respective functions and contributions to swarm coordination and navigation.

Table 2. Swarm system architecture

System Layer	System Function	Importance in Swarm
Perception Layer	Acquisition of distance, orientation, and odometry data	Enables robots to perceive real-world environments
Networking Layer	Peer-to-peer ESP-NOW Mesh data transmission	Ensures multi-agent Internet of Things (IoT) coordination
Decision Layer	Determination of movement direction, formation, and navigation path	Generates collective swarm behavior
Actuation Layer	PWM-based motor control and physical motion execution	Implements navigation decisions in the physical domain

Figure 1. Internet of Things (IoT)-based swarm robot system architecture

Figure 1 illustrates the operational workflow of the proposed IoT-based swarm robot architecture, which progresses from perception to physical actuation. At the perception layer, each robot acquires environmental information such as obstacle distance, heading orientation, and odometry data obtained from ultrasonic sensors, an IMU, and wheel encoders. These data are processed by the ESP32 microcontroller, which serves as the main computational unit and simultaneously functions as an IoT communication node. Position, heading, and navigation status information are then encapsulated into ESP-NOW packets and broadcast in a peer-to-peer manner through the inter-robot mesh network. At the formation control layer, each node receives packets from neighboring robots to compute distance and angular errors relative to the desired formation, enabling navigation decisions to be adjusted collectively and in a fully distributed manner without reliance on a centralized controller. The resulting control outputs are subsequently translated at the actuation layer into PWM signals that drive the DC motors, producing synchronized and adaptive physical motion. This architecture facilitates robust swarm behavior by ensuring that the failure of a single robot does not disrupt overall coordination, while also providing a strong foundation for scalable, low-latency IoT-based swarm robotic systems for indoor navigation.

2.2 Hardware configuration

Each robot was designed using a differential-drive acrylic/3D-printed chassis, as this configuration provides mechanical stability, ease of control, and energy efficiency. The ESP32 microcontroller was selected as the main

processing unit due to its native support for the ESP-NOW protocol, high computational performance, and low power consumption, which are well suited for mobile IoT-based robotic systems. A detailed summary of the hardware components and their functional roles in the swarm robot platform is presented in Table 3.

The physical dimensions of each robot platform are approximately 18 cm × 16 cm × 10 cm with a total weight of around 0.9 kg. The maximum linear velocity of the robot is approximately 0.4 m/s. Each ESP32 node operates with a 240 MHz dual-core processor and transmits data packets with an average payload size of approximately 250 bytes. These parameters ensure sufficient processing capability and communication speed for real-time swarm coordination.

Table 3. Hardware specification of the swarm robot unit

Component	Technical Function	Impact on Performance
ESP32 Devkit-C	CPU and Wi-Fi/Enhanced Peer-to-Peer Network (ESP-NOW) communication module	Handles control processes, sensor acquisition, and mesh data transmission/reception
HC-SR04 Ultrasonic Sensor	Obstacle sensing	Activates collective swarm avoidance behavior
MPU6050 IMU	Gyroscope and accelerometer	Maintains heading accuracy and orientation stability
Motor Encoder	Distance and odometry measurement	Ensures accurate relative position and formation tracking
TB6612FNG Motor Driver	DC motor control interface	Regulates motor direction, speed, and PWM signals
Li-ion 18650 Battery	Power supply	Supports operational duration of approximately 60–120 minutes

The main hardware components integrated into each swarm robot unit are selected to balance computational performance, energy efficiency, and control stability. The ESP32 Devkit-C serves as the central computational core, providing a dual-core processor with native ESP-NOW support that enables simultaneous real-time control execution and peer-to-peer communication. The HC-SR04 ultrasonic sensor is employed as the primary obstacle detection device to trigger collective avoidance behavior, allowing the swarm to synchronously adapt its navigation path when obstacles are detected by any robot. The MPU6050 IMU supplies orientation data, including heading and angular motion, which is essential for maintaining directional stability and formation consistency during movement. Motor encoders mounted on each drive wheel measure actual travel distance and relative positional error, enabling precise odometry-based formation correction. The TB6612FNG motor driver functions as the actuation interface that regulates PWM signals, rotation direction, and speed of the DC motors in accordance with swarm control commands. Power is supplied by a Li-ion 18650 battery, which supports continuous operation for approximately 60 to 120 minutes, allowing sufficiently long indoor experimental sessions without power interruptions. Overall, this hardware configuration is designed to achieve a balanced trade-off between processing capability, power efficiency, and motion control reliability, which are critical factors for successful implementation of IoT-based swarm robotic systems.

Figure 2 presents the physical layout of a single swarm robot unit used in the experiments. The robot adopts a differential-drive configuration with two primary drive wheels and one passive caster wheel, providing mechanical stability and simplifying linear and rotational motion control. The ESP32 module is mounted on the upper section of the chassis as the main computational and communication unit, interconnected with the ultrasonic sensor and IMU through structured wiring to minimize signal interference and facilitate system maintenance. The ultrasonic sensor is positioned at the front of the robot to enable early obstacle detection, while the IMU is placed near the robot's center of mass to improve orientation measurement accuracy. DC motors with integrated encoders are symmetrically installed on the left and right sides of the chassis to maintain torque balance and support precise odometry calculations. This physical arrangement optimizes weight distribution, directional stability, and seamless integration of ESP-NOW communication modules, enabling each robot to operate as an autonomous mobile IoT node capable of participating effectively in mesh-based swarm coordination.

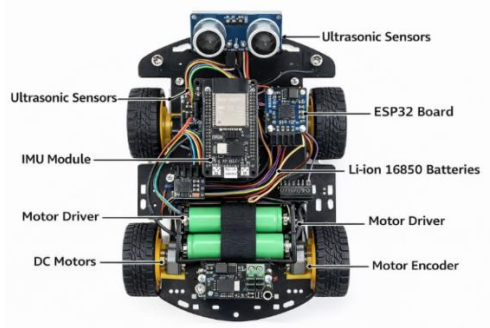

Figure 2. Physical appearance of the swarm robot unit

2.3 Internet of Things communication layer (ESP-NOW Mesh)

Inter-robot communication in the proposed system does not rely on routers or internet connectivity. Instead, it employs ESP-NOW Mesh, which enables direct peer-to-peer data exchange among robots. This approach allows fast, energy-efficient, and stable communication even as the number of swarm nodes increases. The communication characteristics of ESP-NOW and conventional Wi-Fi in the context of indoor swarm robotics applications are compared in Table 4.

Table 4 highlights the advantages of ESP-NOW over conventional Wi-Fi for indoor swarm robotics. ESP-NOW does not require an access point, enabling a fully decentralized and infrastructure-free mesh network that aligns well with the autonomous nature of swarm systems. In terms of latency, ESP-NOW maintains an average transmission delay within the range of 10–25 ms, which is significantly lower than conventional Wi-Fi, where latency may exceed 100 ms as the number of connected clients increases. Low latency is a critical factor in preserving motion synchronization and formation stability within a swarm. Furthermore, ESP-NOW supports lightweight multi-node communication and remains

stable as the number of robots increases, whereas conventional Wi-Fi tends to experience network congestion and overload when the number of clients exceeds approximately ten devices. From an energy consumption perspective, ESP-NOW is also more efficient because it does not require complex network association procedures, making it particularly suitable for battery-powered mobile robotic platforms. Overall, these characteristics make ESP-NOW a more appropriate communication protocol for IoT-based indoor swarm robot implementations compared to conventional Wi-Fi.

Table 4. Hardware communication set

Enhanced Peer-to-Peer Network (ESP-NOW)	Conventional Wi-Fi
No access point required	Dependent on access point
Low latency (10–25 ms)	Latency can exceed 100 ms
Lightweight support for multiple nodes	Prone to overload beyond ~10 clients
Minimal power consumption	High power consumption

Each robot periodically transmits its status information to neighboring nodes, enabling the formation of collective awareness across the swarm. The transmitted packet structure consists of the following fields: node identifier, role, positional coordinates, heading orientation, motion speed, RSSI, and timestamp.

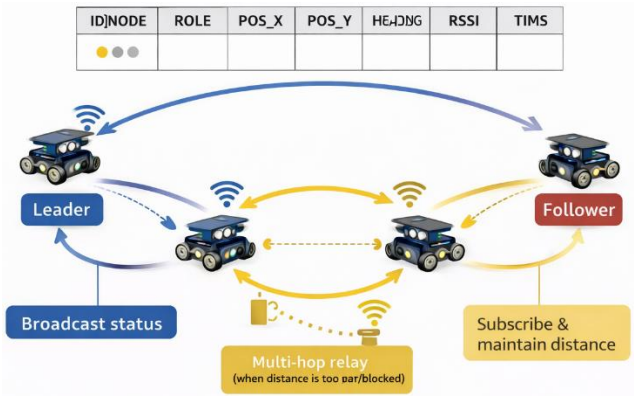

Figure 3. Mesh routing architecture and communication packet flow

Shown:

Leader broadcasts status information to synchronize swarm movement

Followers subscribe to the broadcast messages to maintain relative distance and orientation

Multi-hop relaying is employed when direct communication is limited by distance or physical obstructions

Figure 3 illustrates the ESP-NOW mesh routing architecture and the flow of communication packets within the swarm. In this scheme, the leader robot broadcasts its status information to synchronize swarm movement, while follower robots subscribe to these broadcasts to maintain relative distance and orientation. When direct communication is not feasible due to distance or physical obstructions, multi-hop relaying is employed to forward packets through intermediate robots, thereby preserving network connectivity and coordination across the swarm.

Algorithm 1. Enhanced Peer-to-Peer Network (ESP-NOW) Mesh Communication Procedure

1. Leader node broadcasts status packets to neighboring robots.
2. Neighboring robots receive the packet and update their position information.
3. If the RSSI is below a threshold, the packet is relayed through an intermediate robot.
4. Each robot periodically updates its motion parameters based on the received information.
5. The process repeats continuously to maintain synchronized swarm coordination.

2.4 Swarm behavior algorithm

The swarm coordination mechanism adopts a leader–follower distributed control model, in which each follower robot maintains a desired relative distance (D_a) and orientation (θ_a) with respect to the leader or the preceding robot in the formation.

The motion error is computed as follows:

$$E_D = | D_a - D_t |$$
$$E_\theta = | \theta_a - \theta_t |$$

where, D_t and θ_t represent the measured distance and orientation, respectively. Based on the calculated errors, the robot velocity commands are defined as:

$$V_{linear} = K_D \cdot E_D$$
$$V_{angular} = K_\theta \cdot E_\theta$$

where, K_D and K_θ denote proportional control gains for distance and angular correction. When an obstacle is detected, the avoidance behavior is defined as:

$$Avoidance(D_{obs}) = \begin{cases} Turn\ Left/Right, & \text{if } D_{obs} < 25cm \\ Maintain\ Track, & \text{otherwise} \end{cases}$$

The swarm navigation behavior is organized into multiple operational modes, as summarized in Table 5.

Table 5. Swarm navigation modes

Mode	Function
Tracking Mode	Followers maintain formation relative to the leader
Correction Mode	Swarm performs formation correction when the deviation increases
Avoidance Mode	Leader broadcasts obstacle information and updates swarm trajectory
Re-Formation Mode	Swarm reconstructs the desired formation after maneuvering

The navigation modes define the adaptive behavior of the swarm robot coordination system. Tracking Mode represents the normal operating condition, in which each follower maintains its relative distance and orientation with respect to the leader or preceding robot according to the predefined formation. When positional deviations occur due to environmental disturbances, communication latency, or odometry errors, the system automatically transitions to Correction Mode, where formation errors are reduced by adjusting linear and angular velocities of individual robots. Upon obstacle detection—primarily by the leader—the system

enters Avoidance Mode, during which obstacle information is broadcast to all swarm nodes, enabling collective and synchronized trajectory modification. After the obstacle is successfully bypassed and the path becomes clear, the swarm transitions into *Re-Formation Mode* to restore the ideal formation configuration. This multi-mode mechanism enables the swarm to maintain coordination stability and smooth navigation despite dynamic indoor environmental disturbances.

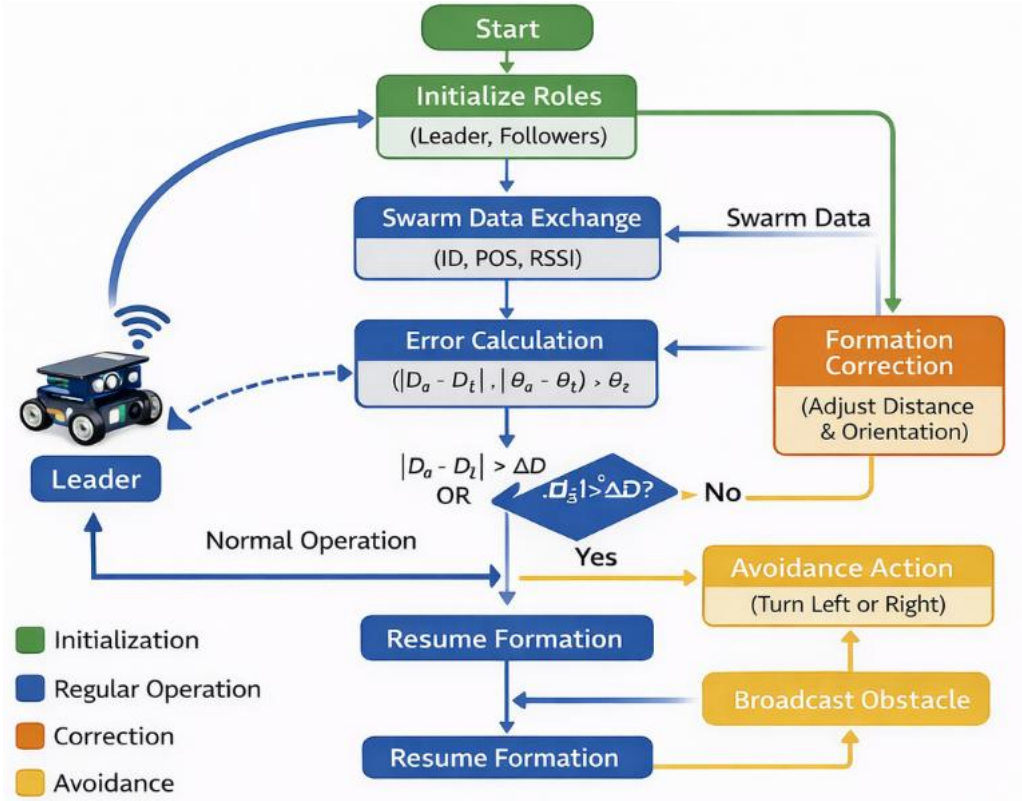

Figure 4. Swarm behavior flowchart

Figure 4 illustrates the logical flow of the swarm robot behavior implemented in this study. The process begins with the Start and Role Initialization stages, during which each robot assigns its role as either leader or follower and initializes formation parameters. During the Data Exchange stage, swarm nodes continuously exchange ESP-NOW packets containing position, orientation, and sensor status information, thereby establishing collective awareness. In the Error Calculation stage, each robot computes distance and angular deviations relative to the desired formation. If the deviation remains within acceptable bounds, minor adjustments are applied during the Correction stage to preserve formation stability. When an obstacle is detected by any node, the system transitions to the Avoidance stage, where navigation trajectories are collectively updated based on broadcast information from the leading robot. Once the obstacle has been avoided, the swarm enters the Resume stage to continue navigation while rebuilding the ideal formation. This control flow ensures adaptive, coordinated, and robust swarm operation in dynamic indoor environments.

2.5 Indoor navigation scenario

The experiments were conducted in a real indoor environment rather than in simulation, allowing signal interference, multipath effects, and physical obstacles to be directly observed and evaluated. The indoor testing scenarios used in this study are summarized in Table 6.

Table 6. Indoor test layout scenarios

Scenario	Path Configuration	Evaluation Objective
S1 — Straight Corridor	Straight corridor (8–12 m)	Initial latency and formation stability
S2 — Obstacle Center	Obstacle placed at the center of the path	Collective avoidance response
S3 — Multi-Room Split	Branched path configuration	Mesh scalability and routing performance

Table 6 describes the indoor environmental scenarios employed for swarm robot experimentation. Scenario S1 (Straight Corridor) represents a straight path with a length of 8–12 meters and is used to observe the baseline performance of the system, particularly initial communication latency and formation stability during unobstructed swarm movement. Scenario S2 (Obstacle Center) introduces one or more obstacles placed along the navigation path to evaluate the swarm's ability to perform collective avoidance, defined as the synchronized response of all robots to obstacle information broadcast by the leading node. Scenario S3 (Multi-Room Split) is designed as a branched path that simulates complex indoor spatial layouts, enabling evaluation of ESP-NOW mesh network scalability as well as multi-hop routing capability in maintaining swarm synchronization. Together, these three scenarios represent varied and realistic indoor conditions for assessing communication reliability, navigation adaptability,

and multi-robot coordination stability under real-world constraints.

The experiments were conducted in an indoor laboratory environment with an approximate area of 10 m × 12 m. The walls are primarily concrete and plaster, which may introduce multipath reflections in wireless signal propagation. In addition, typical laboratory wireless devices such as Wi-Fi routers and laptops may contribute to background radio interference. These environmental factors were considered when analyzing RSSI and latency variations during the experiments.

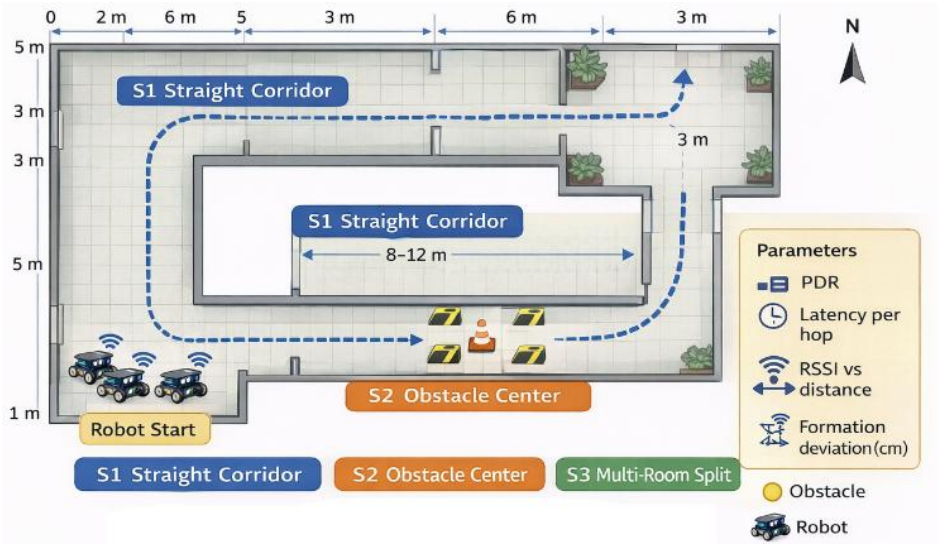

Figure 5. Indoor test environment layout

Figure 5 illustrates the layout of the indoor testing environment used in the swarm robot experiments. The diagram depicts the configuration of straight corridors, branching paths, obstacle locations, and the initial deployment points of the robots for each testing scenario. The layout is designed to represent common indoor environments such as office buildings, laboratories, and storage areas, thereby ensuring high practical relevance of the experimental results. For each test path, the primary performance parameters observed include PDR to assess mesh communication reliability, per-hop latency to measure message propagation speed among nodes, RSSI versus distance to analyze signal strength degradation due to distance and multipath fading, and formation deviation measured in centimeters to evaluate swarm coordination stability. This layout serves as a key reference for correlating communication and navigation performance metrics with the geometric characteristics of different indoor test conditions.

2.6 Performance evaluation method

Performance evaluation was conducted by recording communication packets using a serial logger and a Wi-Fi packet sniffer, followed by quantitative analysis of the collected data. Four primary performance metrics were employed to assess the reliability, responsiveness, and coordination stability of the proposed IoT-based swarm robot system.

1) Packet Delivery Ratio

PDR represents the reliability of the communication network and is defined as:

$$PDR = \frac{Packets_{received}}{Packets_{sent}} \times 100\%$$

2) Communication Latency

Latency measures the time required for a data packet to propagate from the sender to the receiver and is calculated as:

$$Latency = T_{receive} - T_{send}$$

3) Received Signal Strength Indicator Signal Strength Model

The RSSI is modeled as a function of distance using the logarithmic path-loss model: RSSI Signal Strength Model

$$RSSI(d) = RSSI_0 - (10n\log_{10} d)$$

where, RSSI_0 denotes the reference signal strength at a distance of 1 meter, $n$represents the path-loss exponent, and $d$is the distance between communicating nodes.

4) Formation Stability Index

The FSI is introduced to quantify the quality of swarm formation coordination and is defined as:

$$FSI = 1 - \frac{\sum_{i=1}^{N} \quad | E_D |}{N \cdot D_a}$$

where, N is the number of robots in the swarm, E_D represents the distance error for each robot, and D_a denotes the desired inter-robot distance.

The summarized results of the FSI and average positional deviation for different swarm sizes are presented in Table 6. Table 7 presents the FSI and average positional deviation across different swarm sizes. As the number of robots increases, both the average deviation and standard deviation increase, indicating higher coordination complexity and a stronger influence of communication latency and RSSI degradation on formation stability. For the configuration with three robots, an FSI value of 0.958 reflects highly stable

formation control with an average deviation of only 2.1 cm. The FSI value gradually decreases to 0.834 for the seven-robot configuration as the average deviation increases to 8.3 cm. Nevertheless, an FSI value above 0.83 still indicates that the system is capable of maintaining a formation suitable for indoor navigation. These results demonstrate that the proposed ESP-NOW Mesh protocol can sustain stable swarm coordination up to a medium-scale swarm size, despite performance degradation as the number of nodes increases.

Table 7. Summary of Formation Stability Index (FSI) and positional deviation

Number of Robots	Desired Distance (D_a) (cm)	Average Deviation (cm)	Std. Dev. (cm)
3 Robots	50	2.1	0.9
4 Robots	50	3.4	1.2
5 Robots	50	4.9	1.8
6 Robots	50	6.7	2.4
7 Robots	50	8.3	3.1

3. RESULTS

This section presents the experimental evaluation of the proposed IoT-based swarm robot communication system using the ESP-NOW Mesh protocol in an indoor environment. The experiments were conducted under three navigation scenarios: straight corridor (S1), obstacle-centered path (S2), and split-path environment (S3). The performance of the system was assessed using four key metrics: PDR, communication latency, RSSI, and FSI. To ensure statistical reliability, each experiment was repeated five to eight times, and the reported values represent the average results obtained from these trials.

Table 8. Evaluation parameters

Parameter	Scientific Objective	System Relevance
Packet Delivery Ratio (PDR)	Assess mesh communication reliability	Higher PDR indicates better swarm synchronization
Latency	Measure message propagation speed	Lower latency supports stable formation control
Received Signal Strength Indicator (RSSI) Signal Strength	Analyze indoor signal degradation	Evaluates multi-hop routing effectiveness
Formation Stability Index (FSI)	Quantify swarm formation error	Indicator of multi-robot coordination quality

Table 8 presents the key performance metrics used to evaluate the proposed swarm robotic system. These parameters collectively measure communication reliability, network responsiveness, signal propagation characteristics, and swarm coordination stability.

3.1 Packet Delivery Ratio performance

PDR represents the success rate of packet transmission between robots in the swarm. As the proposed system employs peer-to-peer broadcast communication, an increase in the number of nodes leads to higher channel contention and network congestion, which may reduce the number of successfully received packets.

Table 9 presents the average PDR values obtained under three indoor navigation scenarios with varying swarm sizes. For the configuration with three robots, PDR values remain above 98% across all scenarios, indicating that the ESP-NOW Mesh communication provides very high reliability for small-scale swarms. When the swarm size increases to five robots, the PDR slightly decreases but remains above 95%, demonstrating that the system is still able to maintain stable swarm synchronization despite increased broadcast traffic density. For the seven-robot configuration, a more pronounced PDR reduction is observed, particularly in Scenario S3 (split path), which is influenced by increased packet collisions and RSSI degradation caused by multi-hop routing and multipath fading in branched indoor environments. Nevertheless, PDR values above 92% are still considered acceptable for real-time swarm coordination, confirming that the ESP-NOW Mesh protocol remains reliable up to a medium-scale swarm size.

Table 9. Average Packet Delivery Ratio (PDR) results (% over 5–8 trials)

Robots	Scenario	Mean PDR (%)	Std. Dev. (%)
3	**S1**	**99.2**	**0.4**
3	**S2**	**98.6**	**0.5**
3	S3	98.1	0.6
5	S1	97.5	0.8
5	S2	96.8	0.9
5	S3	95.9	1.1
7	S1	95.1	1.3
7	S2	93.7	1.5
7	S3	92.4	1.7

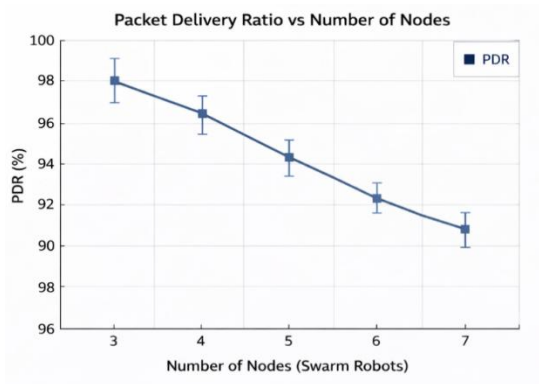

Figure 6. Packet Delivery Ratio (PDR) trend versus number of swarm nodes

Figure 6 illustrates the trend of PDR as the number of robots in the swarm increases. For configurations with three and five robots, PDR values remain consistently high, exceeding 95%, indicating that the ESP-NOW Mesh network maintains reliable communication and stable broadcast synchronization at small to medium swarm scales. Under these conditions, channel contention and packet collisions remain relatively manageable, allowing collective swarm decisions to be executed consistently. As the number of robots increases to seven nodes, a more noticeable decline in PDR is observed, primarily due to increased channel contention, a higher number of broadcast collisions, and multipath fading effects in

complex indoor environments. Despite this degradation, the PDR remains above 92%, which is still sufficient to support real-time swarm coordination.

3.2 Latency analysis in multi-agent communication

Latency is measured as the time difference between packet transmission from the leader robot and reception by follower robots within a single hop. Low latency is a critical requirement for swarm coordination, as propagation delays may cause followers to react late to formation correction commands.

$$Latency = T_{receive} - T_{send}$$

Table 10. Average communication latency

Robots	Scenario	Mean Latency (ms)	Std. Dev. (ms)
3	S1	12.6	1.2
3	S2	14.3	1.5
3	S3	16.8	1.9
5	S1	18.9	2.1
5	S2	22.4	2.5
5	S3	25.7	2.8
7	S1	27.3	3.0
7	S2	32.1	3.5
7	S3	36.8	3.9

Table 10 summarizes the average communication latency measured under three indoor navigation scenarios with different swarm sizes. For the configuration with three robots, latency values range from 12.6 to 16.8 ms, indicating very fast inter-node data exchange that effectively supports real-time swarm coordination. When the swarm size increases to five robots, latency rises to the range of 18.9–25.7 ms, reflecting increased channel contention and the need for multi-hop routing in more complex navigation scenarios. For the seven-robot configuration, latency increases further to 27.3–36.8 ms, particularly in Scenario S3 (split path), due to a higher volume of broadcast packets, intensified multi-hop relaying, and multipath fading effects in indoor environments. Nevertheless, latency values remaining below 40 ms indicate that the system is still capable of maintaining stable coordination and formation correction at a medium swarm scale.

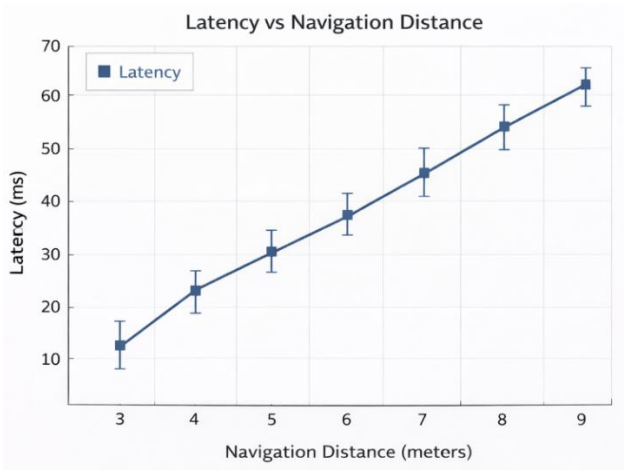

Figure 7. Latency comparison across indoor navigation scenarios

Figure 7 compares communication latency across the three indoor navigation scenarios, namely Straight Corridor (S1), Obstacle Center (S2), and Split Path (S3), for different swarm sizes. Scenario S1 consistently yields the lowest latency because the straight navigation path minimizes multi-hop routing requirements and reduces packet collision probability. In Scenario S2, latency increases due to the presence of physical obstacles that trigger trajectory changes and additional broadcast communication during collective avoidance. Scenario S3 exhibits the highest latency across all swarm configurations, as branched paths significantly increase multi-hop routing requirements and amplify channel contention and multipath fading. These latency variations demonstrate that indoor spatial complexity has a substantial impact on mesh communication performance and directly influences the stability of swarm coordination during navigation.

3.3 Received Signal Strength Indicator degradation over indoor distance

RSSI measurements were conducted to evaluate the degradation of ESP-NOW signal strength as a function of inter-robot distance in indoor environments. The RSSI behavior is modeled using the logarithmic path-loss model:

$$RSSI(d) = RSSI_0 - (10n\log_{10} d)$$

Table 11. Received Signal Strength Indicator (RSSI) versus indoor distance

Distance (m)	Average Received Signal Strength Indicator (RSSI) (dBm)
1 m	−38
3 m	−52
5 m	−63
8 m	−72
10 m	−81

Table 11 presents the relationship between inter-robot distance and the RSSI in an indoor environment. The results show a consistent degradation of RSSI as distance increases, from −38 dBm at 1 meter to −81 dBm at 10 meters. This decreasing trend reflects the typical characteristics of indoor wireless signal propagation, which is strongly influenced by multipath fading, wall reflections, and the presence of physical obstacles. An RSSI level of approximately −80 dBm at a distance of 10 meters indicates that ESP-NOW communication can still be maintained near the effective indoor range limit, albeit with a reduced signal margin. This RSSI degradation correlates with the observed increase in latency and reduction in PDR for larger swarm configurations, thereby highlighting the importance of multi-hop routing mechanisms in preserving mesh communication continuity among robots. These results suggest that the practical communication range of ESP-NOW in indoor swarm environments lies within approximately 8–10 meters, making multi-hop routing a critical requirement for reliable swarm connectivity.

Figure 8 illustrates the RSSI degradation curve as a function of inter-robot distance in an indoor environment. The signal strength decreases in a logarithmic manner as distance increases, which is a common characteristic of radio wave propagation in enclosed spaces affected by multipath fading and wall reflections. At distances below 5 meters, RSSI degradation remains relatively moderate, allowing peer-to-

peer communication to operate with a sufficient signal margin. However, as the distance increases to 8–10 meters, RSSI values decline sharply toward the receiver sensitivity threshold of the ESP-NOW module. Under these conditions, the probability of packet loss increases, and multi-hop routing becomes necessary to maintain mesh communication reliability. This curve confirms that inter-robot spacing and swarm topology are critical factors in sustaining network stability and multi-robot coordination performance in indoor environments.

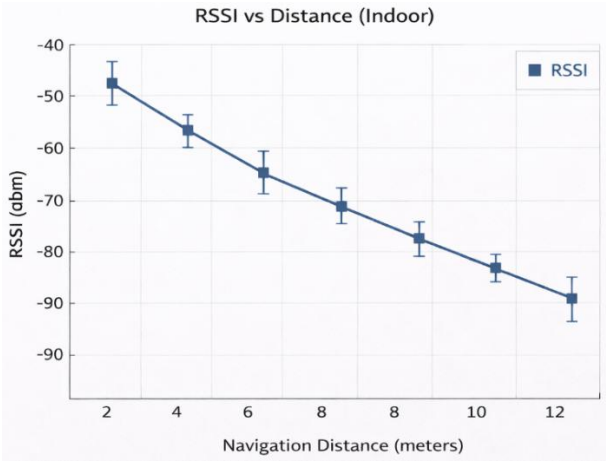

Figure 8. Received Signal Strength Indicator (RSSI) degradation curve as a function of distance

3.4 Formation Stability Index

The FSI is used to quantify the ability of the swarm to maintain the desired inter-robot distance during navigation. FSI provides a normalized measure of formation quality by capturing the cumulative deviation of relative distances among swarm members.

$$FSI = 1 - \frac{\sum_{i=1}^{N} \quad | E_D |}{N \cdot D_a}$$

where, E_D represents the distance error between the actual and desired inter-robot distance, N is the number of robots in the swarm, and D_a is the desired formation distance. FSI values above 0.85 indicate highly stable formations, while values between 0.70 and 0.85 represent moderate stability.

Table 12. Formation error and stability index

Number of Robots	Ideal Distance (cm)	Avg. Formation Error (cm)	Formation Stability Index (FSI)
3 Robots	20	0.9	0.955
5 Robots	20	1.8	0.910
7 Robots	20	3.2	0.840

Table 12 presents the FSI and average formation error for different swarm sizes. As the number of robots increases, the average formation error rises from 0.9 cm for the three-robot configuration to 3.2 cm for the seven-robot configuration. This increase correlates with higher communication latency and RSSI degradation, which affect synchronization accuracy among robots. Despite this trend, the FSI values for all configurations remain within the stable to highly stable range, with values of 0.955 for three robots, 0.910 for five robots, and 0.840 for seven robots. These results demonstrate that the ESP-NOW Mesh-based swarm system is capable of maintaining acceptable formation stability at small to medium swarm scales and confirm the effectiveness of the proposed formation correction mechanism for indoor navigation.

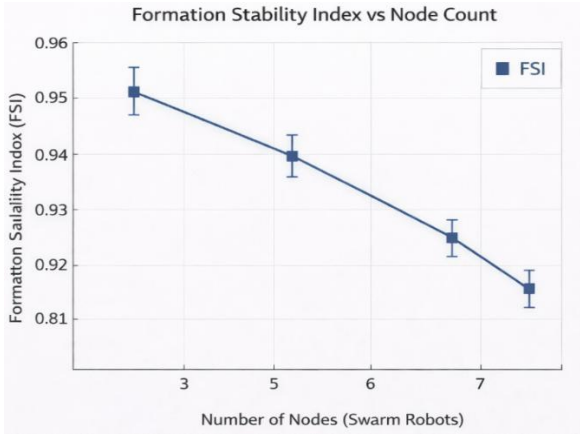

Figure 9. Formation Stability Index (FSI) versus number of swarm nodes

Figure 9 illustrates the trend of FSI as a function of the number of robots in the swarm. The FSI decreases gradually from 0.955 for the three-robot configuration to 0.840 for the seven-robot configuration. This decline reflects the increasing coordination complexity and accumulation of relative position errors caused by RSSI degradation, higher communication latency, and increased packet collisions within the mesh network. Nevertheless, all FSI values remain within the stable to highly stable categories, indicating that the system consistently preserves swarm formation integrity at small to medium scales. This trend confirms that the ESP-NOW Mesh-based formation control strategy effectively maintains coordinated multi-robot behavior in dynamic indoor environments.

3.5 Discussion of swarm communication performance

Based on the overall experimental results, it can be concluded that ESP-NOW Mesh provides a reliable communication backbone for IoT-based swarm robotic systems operating in indoor environments. The system demonstrates high stability for swarm configurations consisting of three to five robots, while the seven-robot configuration begins to exhibit increased network load, reflected in reduced PDR and increased communication latency. Nevertheless, these degradations remain within acceptable tolerance limits for real-time swarm coordination. The consistently low latency values enable responsive multi-agent formation control, ensuring timely correction of relative position and orientation among robots. Although RSSI degradation becomes more pronounced as inter-robot distance and swarm size increase, the implemented multi-hop routing mechanism effectively maintains communication continuity across the swarm. This capability is particularly important in complex indoor layouts where multipath fading and physical obstructions are unavoidable. Furthermore, the FSI results confirm that the swarm is able to preserve formation integrity throughout navigation tasks, even under increased

communication stress. The combined evaluation of PDR, latency, RSSI, and FSI demonstrates that communication performance and formation stability are strongly coupled, and that ESP-NOW Mesh is capable of supporting coordinated swarm behavior in realistic indoor conditions.

3.6 Novelty and contribution analysis

The novelty of this research lies in the experimental implementation of an IoT-based swarm robotic system operating in indoor environments using ESP-NOW Mesh communication. Unlike many previous studies that rely primarily on simulations or experiments involving static IoT nodes, this work presents a fully implemented mobile swarm robot platform evaluated under realistic indoor conditions. This real-world experimental validation provides stronger empirical evidence regarding communication reliability and coordination performance in practical swarm robotic systems. Furthermore, the study performs a comprehensive evaluation using four key performance parameters, namely PDR, communication latency, RSSI signal strength, and FSI. This multi-parameter evaluation enables a more complete understanding of system behavior by simultaneously analyzing communication reliability, network responsiveness, signal propagation characteristics, and swarm coordination stability. The scalability of the proposed system is also demonstrated through experiments involving up to seven swarm robots, which remains relatively uncommon in ESP-NOW-based mobile swarm robotics research. In addition, this study introduces the FSI as a quantitative metric to measure formation integrity and coordination quality in multi-robot systems. The proposed metric provides a normalized and intuitive indicator that can be reused in future swarm robotics studies. Overall, these contributions demonstrate that ESP-NOW Mesh is a lightweight and promising communication framework for infrastructure-free IoT-based swarm robotic systems in indoor environments. Compared with previous swarm communication studies that mainly rely on Wi-Fi or Bluetooth-based networks, the proposed ESP-NOW Mesh approach offers a simpler infrastructure-free architecture with lower latency and energy consumption.

4. CONCLUSION

This study successfully implemented an IoT-based swarm robotic system using the ESP-NOW Mesh communication protocol for multi-agent indoor navigation without reliance on external network infrastructure such as routers or access points. The proposed distributed architecture enables each robot to exchange position, orientation, and navigation status data in real time, allowing the swarm to maintain synchronized leader–follower formations during motion. Experimental results demonstrate that the system achieves very high communication reliability for small to medium swarm configurations. For three and five robots, the PDR remains above 98% and 95%, respectively, across all navigation scenarios. In the seven-robot configuration, PDR decreases to approximately 92–95%, reflecting increased network load, yet remains within acceptable limits for real-time swarm coordination. Communication latency ranges from 12.6–16.8 ms for three robots and 18.9–25.7 ms for five robots, increasing to 27.3–36.8 ms for seven robots. Importantly, all latency values remain below the 40 ms threshold, ensuring responsive formation control and stable multi-agent coordination. RSSI measurements indicate that the practical communication range of ESP-NOW in indoor environments lies within approximately 8–10 meters, with signal strength values between −72 and −81 dBm at longer distances. Despite signal degradation caused by multipath fading and physical obstructions, the implemented multi-hop mesh routing mechanism effectively preserves communication continuity. Formation stability evaluation further confirms robust swarm coordination, with FSI values of 0.955 for three robots, 0.910 for five robots, and 0.840 for seven robots, corresponding to stable to highly stable formation categories. Overall, these findings confirm that ESP-NOW Mesh represents a lightweight, energy-efficient, and reliable IoT communication protocol for indoor swarm robotic systems at small to medium scales. The proposed system shows strong potential for practical applications such as warehouse automation, indoor mapping, assistive robotics, and search-and-rescue operations in infrastructure-limited environments. Future work will focus on scaling the swarm size, integrating vision-based sensing, and incorporating adaptive coordination algorithms based on machine learning to further enhance system intelligence, scalability, and robustness in dynamic real-world conditions.

REFERENCES

[1] Ghanem, R., Ali, I.M., Kasmarik, K., Garratt, M. (2025). Simulation-based multi-objective optimization for mission specific tuning of swarming robots. Swarm and Evolutionary Computation, 99: 102215. https://doi.org/10.1016/j.swevo.2025.102215

[2] Puzicha, A., Buchholz, P. (2021). Decentralized model predictive control for autonomous robot swarms with restricted communication skills in unknown environments. Procedia Computer Science, 186: 555-562. https://doi.org/10.1016/j.procs.2021.04.176

[3] Kumari, N., Lee, K., Ranaweera, C. (2026). Visually extracting the network topology of drone swarms. Robotics and Autonomous Systems, 198: 105313. https://doi.org/10.1016/j.robot.2025.105313

[4] Castellucci, T., Tappia, E., Moretti, E., Melacini, M. (2025). Performance analysis of multi-tote storage and retrieval autonomous mobile robot systems through agent-based simulation. IFAC-PapersOnLine, 59(10): 2533-2538. https://doi.org/10.1016/j.ifacol.2025.09.426

[5] Kviesis, A., Komasilovs, V., Ozols, N., Zacepins, A. (2023). Bee colony remote monitoring based on IoT using ESP-NOW protocol. PeerJ Computer Science, 9: e1363. https://doi.org/10.7717/peerj-cs.1363

[6] Oguz, S., Heinrich, M.K., Allwright, M., Zhu, W.X., Wahby, M., Garone, E. (2024). An open-source UAV platform for swarm robotics research: Using cooperative sensor fusion for inter-robot tracking. IEEE Access, 12: 43378-43395. https://doi.org/10.1109/ACCESS.2024.3378607

[7] Ligot, A., Birattari, M. (2022). On using simulation to predict the performance of robot swarms. Scientific Data, 9: 788. https://doi.org/10.1038/s41597-022-01895-1

[8] Liang, Z., Cao, J.N., Jiang, S., Saxena, D., Chen, J.L., Xu, H.F. (2022). From multi-agent to multi-robot: A scalable training and evaluation platform for multi-robot reinforcement learning. arXiv preprint

arXiv:2206.09590. https://doi.org/10.48550/arXiv.2206.09590

[9] Andronie, M., Lăzăroiu, G., Iatagan, M., Hurloiu, I., Ștefănescu, R., Dijmărescu, A., Dijmărescu, I. (2023). Big data management algorithms, deep learning-based object detection technologies, and geospatial simulation and sensor fusion tools in the Internet of Robotic Things. ISPRS International Journal of Geo-Information, 12(2): 35. https://doi.org/10.3390/ijgi12020035

[10] Liu, D.B., Ren, F.H., Yan, J., Su, G.X., Gu, W., Kato, S. (2024). Scaling up multi-agent reinforcement learning: An extensive survey on scalability issues. IEEE Access, 12: 94610-94631. https://doi.org/10.1109/ACCESS.2024.3410318

[11] Nguyen, L.V. (2024). Swarm intelligence-based multi-robotics: A comprehensive review. AppliedMath, 4(4): 1192-1210. https://doi.org/10.3390/appliedmath4040064

[12] Deshmukh, R.A., Hasamnis, M.A., Kulkarni, M.B., Bhaiyya, M. (2025). Advancing indoor positioning systems: Innovations, challenges, and applications in mobile robotics. Robotica, 43(7): 2710-2750. https://doi.org/10.1017/S0263574725101872

[13] Shahzad, M.M., Saeed, Z., Akhtar, A., Munawar, H., Yousaf, M.H., Baloach, N.K., Hussain, F. (2023). A review of swarm robotics in a NutShell. Drones, 7(4): 269. https://doi.org/10.3390/drones7040269

[14] Keramat, F., Queralta, J.P., Westerlund, T. (2023). Partition-tolerant and byzantine-tolerant decision making for distributed robotic systems with IOTA and ROS2. IEEE Internet of Things Journal, 10(14): 12985-12998. https://doi.org/10.1109/JIOT.2023.3257984

[15] Busch, C. (2022). Ein ESP-NOW basiertes mesh-netzwerk für smart-home-anwendungen. Doctoral dissertation.

[16] Fadhil, J.A., Zeebaree, S.R.M. (2024). Blockchain for distributed systems security in cloud computing: A review of applications and challenges. Indonesian Journal of Computer Science, 13(2): 1576-1605. http://ijcs.net/ijcs/index.php/ijcs/article/view/3794/473.

[17] Zhang, Y.Q., Abellera, J.U. (2025). Autonomous mobile robotics in smart warehousing: A cyber-physical systems approach to inventory management. Future Technology, 4(4): 59-71. https://doi.org/10.55670/fpll.futech.4.4.6

[18] Sebastian, E., Duong, T., Atanasov, N., Montijano, E., Sagues, C. (2025). Physics-informed multiagent reinforcement learning for distributed multirobot problems. IEEE Transactions on Robotics, 41: 4499-4517. https://ieeexplore.ieee.org/stamp/stamp.jsp?arnumber=11049031.

[19] Siwek, M. (2024). Consensus-based formation control with time synchronization for a decentralized group of mobile robots. Sensors, 24(12): 3717. https://doi.org/10.3390/s24123717

[20] Nitti, A., de Tullio, M.D., Federico, I., Carbone, G. (2025). A collective intelligence model for swarm robotics applications. Nature Communications, 16: 6572. https://doi.org/10.1038/s41467-025-61985-7

[21] Cruz, M., Mafra, S., Teixeira, E., Figueiredo, F. (2022). Smart strawberry farming using edge computing and IoT. Sensors, 22(15): 5866. https://doi.org/10.3390/s22155866

[22] Zhang, T.Y., Xue, C.Y., Wang, J.C., Yun, Z.L., Lin, N.T., Han, S. (2024). A survey on Industrial Internet of Things (IIoT) Testbeds for connectivity research. arXiv preprint arXiv:2404.17485. https://doi.org/10.48550/arXiv.2404.17485

[23] Phadke, A., Antonio Medrano, F., Sekharan, C.N., Chu, T.X. (2024). An analysis of trends in UAV swarm implementations in current research: Simulation versus hardware. Drone Systems and Applications, 12: 1-10. https://doi.org/10.1139/dsa-2023-0099

[24] Tota, P., Tirian, G.O., Vaida, M.F., Maris, S.D., Terebes, R.M. (2023). Mesh network with telepresence robots for advertising. In 2023 IEEE 17th International Symposium on Applied Computational Intelligence and Informatics (SACI), Timisoara, Romania, pp. 000793-000800. https://doi.org/10.1109/SACI58269.2023.10158608

[25] Thanh, V.N., Vinh, D.P., Tho, N.V., Duc, T.Q., Minh, N.L. (2024). Application of bluetooth mesh network in multi-device system management. University of Danang - Journal of Science and Technology, 22(3): 7-12. https://doi.org/10.31130/ud-jst.2024.540E

[26] Zhang, S.Q., Ma, Y., Tafazolli, R. (2025). Robot subset selection-based multi-user edge computing for swarm lifetime maximization with correlated data sources. Engineering. 56: 173-185. https://doi.org/10.1016/j.eng.2025.10.015

[27] Yang, C., Yu, H., Guo, Q., Taleb, T., Requena, J.C., Tammi, K. (2025). Deterministic networking empowered robotic teleoperation. IEEE Network, 39(4): 280-289. https://doi.org/10.1109/MNET.2024.3483930

[28] Conceição, M.I., Grilo, A., Basiri, M. (2025). Communication and motion coordination awareness in networked aerial robot teams. Ad Hoc Networks, 176: 103875. https://doi.org/10.1016/j.adhoc.2025.103875

[29] Wu, K.F., Hu, J.Y., Ding, Z.T., Arvin, F. (2023). Distributed bearing-only formation control for heterogeneous nonlinear multi-robot systems. IFAC-PapersOnLine, 56(2): 3447-3452. https://doi.org/10.1016/j.ifacol.2023.10.1496

[30] Lu, Q., Miao, Z.Q., Zhang, D., Yu, L., Ye, W.J., Yang, S.X., Su, C.Y. (2019). Distributed leader-follower formation control of nonholonomic mobile robots. IFAC-PapersOnLine, 52(15): 67-72. https://doi.org/10.1016/j.ifacol.2019.11.651

[31] Sinigaglia, C., Manzoni, A., Braghin, F., Berman, S. (2022). Indirect optimal control of advection-diffusion fields through distributed robotic swarms. IFAC-PapersOnLine, 55(30): 299-304. https://doi.org/10.1016/j.ifacol.2022.11.069

[32] Park, S., Lee, S. (2026). A stochastic game theory based energy-efficient device-to-device communication optimization for autonomous mobile robots over industrial IoT networks. Computer Networks, 274: 111864. https://doi.org/10.1016/j.comnet.2025.111864

[33] Krishna, G., Singh, R., Gehlot, A., Shaik, V.A., Twala, B., Priyadarshi, N. (2024). IoT-based real-time analysis of battery management system with long range communication and FLoRa. Results in Engineering, 23: 102770. https://doi.org/10.1016/j.rineng.2024.102770

[34] Rahim, M.A., Rokonuzzaman, M., Alqumsan, A.A., Arogbonlo, A., Islam, M.Z., Trinh, H., Islam, M.S. (2025). An intelligent and secure internet of robotic things: A review and conceptual framework. Internet of Things, 33: 101684. https://doi.org/10.1016/j.iot.2025.101684